# Poly(ADP-ribose) Polymerase-2 (PARP-2) Is Required for Efficient Base Excision DNA Repair in Association with PARP-1 and XRCC1

Valérie Schreiber, Jean-Christophe Amé, Pascal Dollé, Inès Schultz, Bruno Rinaldi, Valérie Fraulob, Josiane Ménissier-de Murcia, Gilbert de Murcia

THE JOURNAL OF BIOLOGICAL CHEMISTRY
Vol. 277, No. 25, Issue of June 21, pp. 23028–23036, 2002

*Printed in U.S.A.*

# Poly(ADP-ribose) Polymerase-2 (PARP-2) Is Required for Efficient Base Excision DNA Repair in Association with PARP-1 and XRCC1*

Received for publication, March 12, 2002, and in revised form, April 8, 2002
Published, JBC Papers in Press, April 10, 2002, DOI 10.1074/jbc.M202390200

**Valérie Schreiber‡, Jean-Christophe Amé‡, Pascal Dollé§, Inès Schultz‡, Bruno Rinaldi‡, Valérie Fraulob§, Josiane Ménissier-de Murcia‡, and Gilbert de Murcia‡¶**

*From the ‡UPR 9003 du Centre National de la Recherche Scientifique, Laboratoire conventionné avec le Commissariat à l'Energie Atomique, Université Louis Pasteur, Ecole Supérieure de Biotechnologie de Strasbourg, boulevard Sébastien Brant, F-67400 Illkirch and the §Institut de Génétique et de Biologie Moléculaire et Cellulaire, CNRS/INSERM/ULP, Collège de France, BP 163, 67404 Illkirch cedex, France*

**The DNA damage dependence of poly(ADP-ribose) polymerase-2 (PARP-2) activity is suggestive of its implication in genome surveillance and protection. Here we show that the PARP-2 gene, mainly expressed in actively dividing tissues follows, but to a smaller extent, that of PARP-1 during mouse development. We found that PARP-2 and PARP-1 homo- and heterodimerize; the interacting interfaces, sites of reciprocal modification, have been mapped. PARP-2 was also found to interact with three other proteins involved in the base excision repair pathway: x-ray cross complementing factor 1 (XRCC1), DNA polymerase β, and DNA ligase III, already known as partners of PARP-1. XRCC1 negatively regulates PARP-2 activity, as it does for PARP-1, while being a polymer acceptor for both PARP-1 and PARP-2. To gain insight into the physiological role of PARP-2 in response to genotoxic stress, we developed by gene disruption mice deficient in PARP-2. Following treatment by the alkylating agent *N*-nitroso-*N*-methylurea (MNU), PARP-2-deficient cells displayed an important delay in DNA strand breaks resealing, similar to that observed in PARP-1 deficient cells, thus confirming that PARP-2 is also an active player in base excision repair despite its low capacity to synthesize ADP-ribose polymers.**

In response to DNA interruptions, PARP-1,[1] the founding member of the poly(ADP-ribose) polymerase superfamily, catalyzes the successive covalent addition of ADP-ribose units from NAD to a limited number of nuclear acceptors to form a branched anionic polymer. PARP-1 is a nuclear enzyme involved in the detection and signaling of DNA strand breaks introduced either directly by ionizing radiation or indirectly following enzymatic incision of a DNA lesion (abasic sites or oxidized or alkylated bases) repaired by the base excision repair (BER) pathway (see for review Ref. 1). The discovery of numerous PARP-1 protein partners and/or poly(ADP-ribose) acceptors involved in DNA architecture (histones H1 and H2B, lamin B, and high mobility group proteins) or in DNA metabolism (DNA replication factors, DNA repair proteins, *i.e.* XRCC1, transcription factors, topoisomerases, and PARP-1 itself) has shed light onto the implication of PARP-1 in these processes (see for review Ref. 1).

The function of PARP-1 in BER has long been assumed, until direct evidence demonstrated the presence of PARP-1 in the BER complex, associated to XRCC1 (2, 3) and DNA polymerase (pol) β (4). The polymer produced by PARP-1 upon activation by DNA breaks triggers the recruitment of XRCC1, which shows high affinity for oligo(ADP-ribosyl)ated PARP-1 (3–5). The requirement of PARP-1 in BER was established *in vivo*, because PARP-1 knock-out cells displayed a severe defect in strand breaks resealing following genotoxic treatment (6, 7). The preferential role of PARP-1 in long patch BER was observed using extracts from these PARP-1 knock-out cells (4). Photoaffinity labeling experiments revealed that PARP-1 binds to BER intermediates (8). In reconstituted *in vitro* systems containing purified human BER enzymes, PARP-1 was shown to stimulate strand displacement DNA synthesis by DNA polβ, in cooperation with FEN-1, leading to long patch BER (9).

The mouse models in which the PARP-1 gene has been knocked out (10–12) revealed the dual facets of PARP-1 function. In proliferative cells inflicted with sub-lethal doses of DNA damage, PARP-1 as a survival factor participates in DNA damage detection and signaling, leading to cell cycle arrest and DNA repair, to avoid deleterious genetic alterations (1). On the other hand, in post-mitotic cells, massive DNA damage as observed in pathological conditions such as cerebellar or cardiac ischemia or septic shock and to overactivate PARP-1, triggering energy depletion that leads to cell death (see for review Ref. 13).

The PARP-1 knock-out mice were at the origin of the discovery of a new DNA damage-dependent PARP protein, named PARP-2, because an unexpected residual poly(ADP-ribose) synthesis could be measured in PARP-1-deficient cells following DNA damage (14, 15). In addition to PARP-2 (15–17), several other PARPs were discovered almost simultaneously, all having in common a conserved catalytic domain responsible for poly(ADP-ribose) synthesis: PARP-3 (17), vPARP, a 193-kDa PARP belonging to the vault particles (18), Tankyrase 1 and 2, two proteins associated to the telomeric protein TRF1 but also found in the Golgi or in nuclear pore complexes (19–22), and the 2,3,7,8-tetrachlorodibenzo-*p*-dioxin-inducible TiPARP (23).

* This work was supported by Association pour la Recherche Contre le Cancer, Ligue Nationale contre le Cancer et Comité Régional, Electricité de France, Commissariat à l'Energie Atomique and Centre National de la Recherche Scientifique. The costs of publication of this article were defrayed in part by the payment of page charges. This article must therefore be hereby marked "*advertisement*" in accordance with 18 U.S.C. Section 1734 solely to indicate this fact.

¶ To whom correspondence should be addressed. Tel.: 33-390-24-47-07; Fax: 33-390-24-46-86; E-mail: demurcia@esbs.u-strasbg.fr.

[1] The abbreviations used are: PARP, poly(ADP-ribose) polymerase; 3-AB, 3-aminobenzamide; APE1, apurinic/apyrimidinic endonuclease 1; BER, base excision repair; BRCT, BRCA1 C-terminus; d.p.c., days postcoitum; dRP, deoxyribose phosphate; EST, expressed sequence tags; FEN-1, flap endonuclease-1; GFP, green fluorescence protein; GST, glutathione *S*-transferase; h, human; m, mouse; SPR, short patch repair; LPR, long patch repair; MEF(s), mouse embryonic fibroblast(s); MNU, *N*-nitroso-*N*-methylurea; PNK, polynucleotide kinase; pol, polymerase; XRCC1, x-ray cross complementing factor 1; E, embryonic day.

PARP-1 and PARP-2 are the only ones reported to be DNA damage-dependent, and in *Arabidopsis thaliana* both *PARP-1* and *PARP-2* genes are induced by ionizing radiation (24). The N-terminal part of mammalian PARP-2 contains a nuclear location signal and a functional DNA binding domain (15) distinct from that of PARP-1 (two zinc fingers). The nature of this DNA binding domain has yet to be determined.

In our attempts to further characterize PARP-2 and compare its biological implication with that of PARP-1 with respect to DNA damage surveillance, we discovered that the expression pattern of PARP-2 and PARP-1 genes follows almost the same tissue distribution. The two proteins homo- and heterodimerize and poly(ADP-ribosyl)ate each other. In addition, PARP-2 was found to interact with the BER proteins XRCC1, DNA pol$\beta$, and DNA ligase III, all being PARP-1 partners as well. XRCC1 could be heteromodified by PARP-2 and was able to negatively regulate PARP-2 activity as it does for PARP-1. The requirement for PARP-2 in BER was demonstrated *in vivo* by the COMET assay in mouse embryonic cells lacking PARP-2. Our results showed that PARP-2 is a component of a functional BER complex *in vivo*, likely through dimerization with PARP-1. This strengthens the role of PARP-2 as a survival factor following genotoxic stress.

## EXPERIMENTAL PROCEDURES

*Plasmids*—The *Sma*I/*Not*I fragment encoding full-length murine PARP-2 (mPARP-2) cDNA was isolate from pVL-mPARP-2 (15), and sub-cloned into *Hpa*I/*Not*I sites of the pBC vector (25) in-frame with GST, allowing the expression of GST-mPARP-2 fusion protein. Truncated forms of mPARP-2 were generated by PCR and cloned in-frame with GST in the pBC vector. The *Xho*I/*Xho*I PCR product encompassing full-length mPARP-2 was ligated into the *Xho*I site of pEGFP-C3 vector (CLONTECH, Palo Alto, CA), allowing the expression of GFP-mPARP-2. Complementary oligonucleotides encoding the FLAG epitope following a methionine were linked into the *Eco*RV/*Eco*RI sites of the pIRES-eGFP vector (CLONTECH), allowing the expression of the FLAG epitope (F). The cDNA encoding full-length human XRCC1 (hXRCC1, kindly given by K. Caldecott) was subcloned into the EcoRI sites of pIRES-FLAG vector, allowing the expression of FLAG-tagged XRCC1 (F-hXRCC1).

*In Situ Hybridization*—*In situ* hybridization was performed as described in Niederreither and Dollé (26) on serial sections (10 $\mu$m) of frozen embryos or mouse adult organs dissected from 2- or 16-week CD1 mice and frozen in OCT. A *Xho*I/*Pst*I fragment from a mouse PARP-1 EST clone (AA032357, Research Genetics, Huntsville, AL), encoding residues 337–572, was subcloned into pBluescript SK(+), and antisense and sense mPARP-1 riboprobes were produced using T3 and T7 RNA polymerases, respectively. The murine PARP-2 probe corresponding to residues 8–363 is described in Amé *et al.* (15). Exposure varied from 4 to 6 weeks for PARP-1 and PARP-2 probes.

*Immunoprecipitation, GST Pull-down, and Western Blot Analyses*—For immunoprecipitation of purified proteins, 1 $\mu$g of purified hPARP-1 and/or mPARP-2 (as indicated) was incubated 2 h at 4 °C with 20 $\mu$l of F1.23 monoclonal anti-PARP-1 antibody and 1 $\mu$g of bovine serum albumin in 1 ml of LSB (20 mM Tris-HCl pH 8, 120 mM NaCl, 0.1% Nonidet P-40, 0.5 mM phenylmethylsulfonyl fluoride) with protease inhibitors (Complete Mini, Roche Molecular Biochemicals, Mannheim, Germany). Protein G-Sepharose beads (Amersham Biosciences, Inc.) were added, and after 30-min incubation at 4 °C, bound immune complexes were washed three times with LSB buffer, and the pellets were resuspended in Laemmli buffer and heated 3 min at 100 °C before analysis by Western blotting. For immunoprecipitation of endogenous PARP-1 from HeLa cells, cells were lysed in LSB buffer 20 min at 4 °C, scraped, and centrifuge 20 min at 13,000 rpm at 4 °C. After preclearing with protein G-Sepharose 30 min at 4 °C, 20 $\mu$l of F1.23 anti-PARP-1 antibody was added, and immunoprecipitation was carried on as described above.

GST-pull-down analyses were performed in HeLa S3 cells as described in Dantzer *et al.* (4).

For immunodetection, blots were incubated with anti-PARP-1 (Monte 1/2,500 (4)), anti-PARP2 (Yuc 1/2,500 (15)), anti-XRCC1 (Roman 1/5,000 (3)), anti-DNA pol$\beta$ (1/1,000 (4)), and anti-DNA ligase III (1/250, kindly given by A. Tomkinson, San Antonio, TX) polyclonal antibodies or with anti-GST (1/10,000, Institut de Génétique et de Biologie Moléculaire et Cellulaire, Illkirch, France) and anti-GFP (1/1000, Roche Molecular Biochemicals, Indianapolis, IN) monoclonal antibodies. Blots where then probed with horseradish peroxidase-coupled secondary antibodies (goat anti-rabbit, 1/20,000 or sheep anti-mouse, 1/20,000, Sigma Chemical Co., St. Louis, MO), and immunoreactivity was detected by enhanced chemiluminescence (PerkinElmer Life Sciences, Boston, MA). When indicated, 3-AB (1 mM) was added 2 h prior to lysis and maintained throughout all the lysis and washing steps.

*Heteromodification of GST Fusion Proteins by PARP-2 or PARP-1*—GST pull-down assays were performed as described above, except that washes were done with HSB (20 mM Tris-HCl, pH 8, 500 mM NaCl, 0.5% Nonidet P-40, 0.5 mM phenylmethylsulfonyl fluoride). After a last wash with activity buffer (50 mM Tris-HCl, pH 8, 4 mM $MgCl_2$, 0.3 mM dithiothreitol), each sample was split onto three, the beads were pelleted (volume of the pellet: $\pm$ 20 $\mu$l) and resuspended in 300 $\mu$l of activity buffer containing either 300 pmol of hPARP-1, 600 pmol of mPARP-2, or no PARP. Reaction was started by the addition of 180 $\mu$l of activity buffer containing DNase I-activated calf thymus DNA, and [$^{32}$P]NAD. Final concentrations were 0.5 $\mu$g of DNA, 1 $\mu$M NAD for control, and PARP-2 and 0.1 $\mu$M for PARP-1 samples. In addition, each sample contained 1 pmol of [$^{32}$P]NAD (1000 Ci/mmol). After 4 min at 25 °C, the reaction was stopped by the addition of 500 $\mu$l of cold HSB on ice, and beads were washed three times with HSB, resuspended in 12 $\mu$l of Laemmli buffer, and heated for 3 min at 100 °C before analysis by Western blot.

*Poly ADP-ribosylation of PARP-2 and XRCC1*—Purified mPARP-2 (200 pmol) was incubated with 1- to 8-fold purified hXRCC1 (3) for 2 min at 25 °C in 40 $\mu$l of activity buffer containing 300 ng of bovine serum albumin, 5 $\mu$M [$^{32}$P]NAD (1000 Ci/mmol), and 100 ng of DNase I activated calf thymus DNA. Reaction was stopped by addition of 15 $\mu$l of Laemmli buffer on ice, and reaction products were analyzed by gel electrophoresis on 8% SDS-PAGE and autoradiography of the Coomassie Blue-stained and dried gel.

*Generation and Culture of Mouse Embryonic Fibroblasts*—Mouse embryonic fibroblasts (MEFs) were isolated by micro-dissection of embryos at day 13.5 of gestation resulting from intercrosses between PARP-2$^{+/-}$ heterozygous mice. Each embryo was genotyped by PCR to screen for the disruption of the PARP-2 allele. The generation of these mice and the genotyping PCR procedure will be described elsewhere. MEFs were maintained in Dulbecco's modified Eagle's medium, 4.5 g/liter glucose medium supplemented with 10% fetal bovine serum and 0.5% gentamicin. For Western blot analysis, $10^5$ cells were resuspended in Laemmli buffer and sonicated, and proteins were analyzed by Western blot as described above, using anti-PARP-2 (Yuc) and anti-PARP-1 (Monte) polyclonal antibodies. The evaluation of residual poly(ADP-ribose) synthesis in MEF cell extracts was performed as described by Amé *et al.* (15).

*Single Cell Gel Electrophoresis (COMET) Assay*—Passage 3 MEFs were thawed 48 h prior to harvesting on 60-mm Petri dishes. The following day, cells were either mock treated or exposed for 30 min to *N*-nitroso-*N*-methylurea (MNU) as indicated. COMET assay was performed as described in Trucco *et al.* (6). Slides were dried in cold ethanol, and DNA was stained prior to scoring with 2 $\mu$g/ml ethidium bromide. Fifty COMET per slide were observed using a Zeiss Axioplan microscope equipped with a DP50 camera (Olympus) and analyzed using the VisCOMET software (Impuls Bildanalyse GmbH, Gilsching, Germany) to calculate the tail moment as defined by Olive *et al.* (27).

## RESULTS

*Tissue Distribution of PARP-1 and PARP-2 Transcripts during Embryogenesis and in Mouse Adult Tissues—In situ* hybridization experiments were performed to compare the expression patterns of the *PARP-1* and *PARP-2* genes at various stages of mouse development and in adult tissues. Antisense probes for PARP-1 and PARP-2 yielded specific labeling patterns that appeared similar although not perfectly identical. During early developmental stages, both genes were expressed throughout the embryo (data not shown). Differential labeling patterns became apparent by E12.5. At that stage, both genes were expressed at high levels in the developing liver and kidney (Fig. 1, *A–C*). Only *PARP-1*, however, was found to be expressed at higher levels in the genital ridge and the spinal ganglia. The signals observed throughout other embryonic regions for both PARP-1 and PARP-2 antisense probes were higher than for the corresponding sense probes (data not shown), indicating a ubiq-

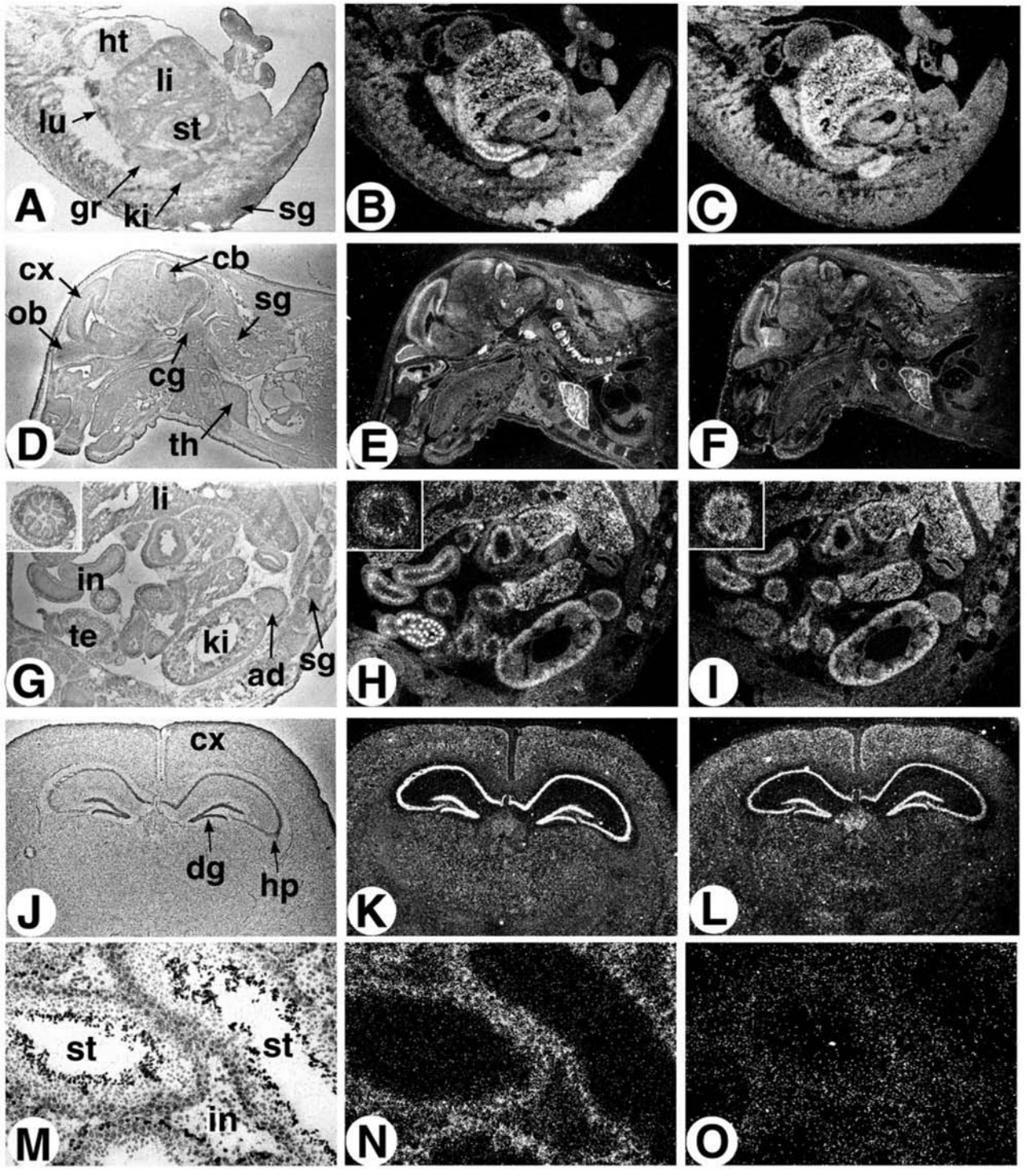


FIG. 1. **Comparative *in situ* analysis of PARP-1 and PARP-2 transcript distributions in mouse embryos and adults organs.** Each row consists of dark-field views of PARP-1 (*middle*) and PARP-2 (*right*) *in situ* hybridization signals (*white dots*) on adjacent sections, and one of the corresponding bright-field views (*left*) to show histological details. Sagittal sections through the trunk region of an E12.5 embryo (*A–C*), the head and neck of an E18.5 fetus (*D–F*), and the abdominal cavity of an E18.5 fetus (*G–I*). The *insets* show an enlargement of one of the intestinal loops. Frontal sections of an adult (16-week-old) mouse brain (*J–L*). Sections through the testis of a 16-week-old male (*M–O*). *ad*, adrenal gland; *cb*, cerebellum; *cg*, cranial ganglia; *cx*, cortex; *dg*, dentate gyrus; *gr*, genital ridge; *hp*, hippocampus; *ht*, heart; *in*, intestinal epithelium (*G*) or interstitial tissue (*M*); *ki*, kidney; *li*, liver; *lu*, lung; *ob*, olfactory bulb; *sg*, spinal ganglia; *st*, seminiferous tubules; *te*, testis; *th*, thymus.

uitous moderate expression of both enzymes.

At E18.5 (Fig. 1, *D–I*), *PARP-1* and to a lesser extent *PARP-2* were preferentially expressed in the thymus and in regions of the nervous system (see below). Within the developing trunk, preferential expression of *PARP-1* and *PARP-2* persisted in the liver and became restricted to the cortical region of the kidney, the spleen, adrenal gland, and in stomach and intestinal epithelia (Fig. 1, *G–I*, and data not shown). Note that PARP-1 transcripts appeared more restricted than those of PARP-2 toward the base of the intestinal crypts (*G–I*, *insets*).

From E14.5 to E18.5, as well as in the adult mouse, both genes were expressed at the highest levels in the thymus (Fig. 1, *D–F* and data not shown). In the adult mouse, *PARP-1* and *-2* expression was particularly high in the subcapsular zone of the

thymus (data not shown), where immature lymphocytes proliferate. Expression decreased as lymphocytes mature and was also found in the medulla. PARP-1, and to a lesser extend, PARP-2 transcripts were detected in the white pulp of the spleen, especially in the germinal centers and in Peyer's patches in the intestine wall (data not shown) suggesting that high levels of *PARP-1* and *-2* expression are related to proliferation of immature lymphocytes.

At E18.5, PARP-1 was preferentially expressed in specific brain regions (see the olfactory bulb, cerebellar, and cerebral cortex in Fig. 1, *D–F*) and in the olfactory epithelia. Expression was also higher in the cranial and spinal ganglia. PARP-2 expression appeared more homogeneous in craniofacial tissues, although it was slightly up-regulated in brain and cranial/spinal ganglia. In the adult brain (Fig. 1, *J–L*), both PARP-1 (28) and PARP-2 genes showed high expression in neuronal cells forming the stratum granulosum of the dentate gyrus and the stratum pyramidale of the hippocampus (CA 1–3). Weaker expression was detected in cells of the cerebral cortex. Only *PARP-1*, however, was expressed at high levels in the Purkinje cell layer of the cerebellum (data not shown).

It is in testis that the expression pattern of *PARP-1* and *PARP-2* is the most distinct. *PARP-1* is expressed at high levels in the seminiferous tubules of the developing testis (Fig. 1, *G–I*). Expression was particularly strong in the basal layers of the seminiferous epithelium (Fig. 1, *M–N*, and Ref. 29), whereas no signal was detected in the luminal layers of the seminiferous epithelium indicating a down-regulation of *PARP-1* expression at the haploid stage of meiosis. In contrast, the PARP-2 signal was weak and rather homogeneous, throughout the seminiferous tubules and the interstitial tissue (Fig. 1*O*).

Apart from testis, the expression pattern of *PARP-2* resembles that of *PARP-1* except that the level of expression of *PARP-2* is weaker.

*PARP-2 and PARP-1 Homo- and Heterodimerize*—PARP-1 is known to act as a catalytic dimer (30, 31). To investigate possible homodimerization of PARP-2, extracts from HeLa cells transfected with a plasmid allowing the overexpression of murine PARP-2 (mPARP-2) in fusion with GST were mixed with extracts from HeLa cells transfected with a plasmid allowing the expression of either mPARP-2 fused to GFP, or GFP alone (Fig. 2, *lanes 2* and *6*, respectively). GST fusion proteins were also generated expressing truncated versions of mPARP-2 (see Fig. 2): amino acids 1–69 (Nt, the DNA binding domain), amino acids 63–202 (domain E), and amino acids 203–559 (F, the catalytic domain). GST-fused proteins were trapped on glutathione-Sepharose beads, and copurifying GFP-tagged mPARP-2 was assessed by Western blot analysis using anti-GFP antibody. Fig. 2 shows that PARP-2 is able to homodimerize (*lane 2*) through its E domain (*lane 4*).

To further investigate the possibility that PARP-2 forms heterodimers with PARP-1 and to prevent any cross-reaction with PARP-2, we immunoprecipitated PARP-1 from HeLa cell extracts using the F1.23-specific monoclonal antibody raised against the N-terminal part of PARP-1 (32). PARP-2 was coimmunoprecipitated with PARP-1 (Fig. 3*A*, *lane 3*). A negative control using an unrelated antibody did not trap either of these two proteins (*lane 2*). The interaction between PARP-2 and PARP-1 was also observed (*lane 4* and see Fig. 5*B* below) in the presence of the PARP inhibitor 3-aminobenzamide (3-AB), indicating that it occurs independently of their polymerizing activity.

The complex between PARP-1 and PARP-2 was reconstituted *in vitro* using purified proteins: mPARP-2 was coimmunoprecipitated with human PARP-1 (hPARP-1) using the F1.23 antibody (Fig. 3*B*, *lane 4*) demonstrating a direct interaction between PARP-2 and PARP-1.

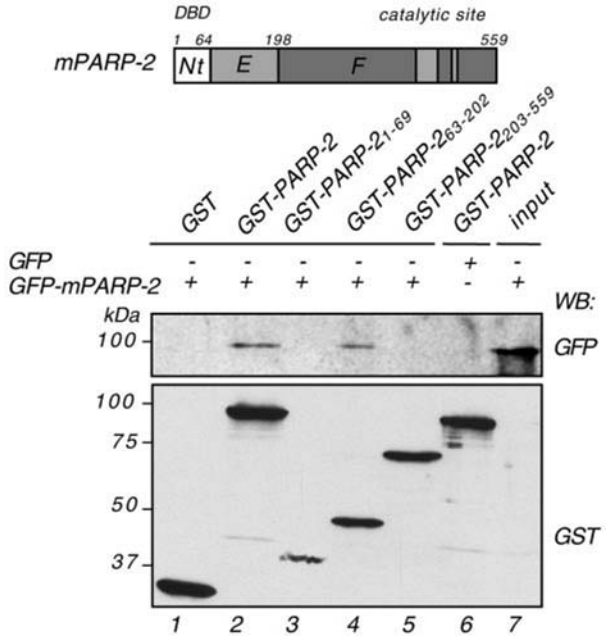


FIG. 2. **PARP-2 homodimerizes.** *Top*: schematic representation of mPARP-2. *DBD*, DNA binding domain. *Bottom*: Extracts from HeLa cells expressing GST (*lane 1*) and GST-tagged mPARP-2 (*lanes 2* and *6*) or deletion mutants of mPARP-2 (*lanes 3–5*) were mixed with extracts from HeLa cells expressing GFP (*lane 6*) or GFP-mPARP-2 (*lanes 1–5*). Interacting proteins were analyzed by GST-pull-down and Western blot with anti-GFP antibody (*top*). Blot was subsequently probed with anti-GST antibody (*bottom*). *Lane 7* (*input*): 1/50 of the total cell extract of HeLa cells transfected with GFP-mPARP-2.

*Identification of the Domains Involved in the Association of PARP-2 with PARP-1*—To map the interaction domain within PARP-1, GST fusion proteins were generated expressing truncated versions of hPARP-1 (Fig. 4*A*): amino acids 1–371 (A–C, the DNA binding domain), amino acids 174–366 (B and C), amino acids 384–524 (D, encompassing the BRCT domain), amino acids 572–1014 (F, encompassing the catalytic domain), and amino acids 525–655 (region E). These fusion proteins were overexpressed in HeLa cells, and GST pull-down experiments were performed followed by Western blot analyses. Copurification of endogenous PARP-2 was efficient with constructs containing either the DNA binding domain (*lane 2*) or the BRCT domain (*lane 4*). These domains are those involved in the homodimerization of PARP-1 (Fig. 4*A* and Ref. 30), as well as in the binding to several partners such as XRCC1 (3), DNA pol$\beta$ (4), DNA ligase III (Fig. 4*A*), histones, hUbc9, and transcription factors such as E47, TEF-1, RXR$\alpha$, Oct-1, and YY1 (see for review Ref. 1), suggesting that the DNA binding and the BRCT domains of PARP-1 are interfaces for protein-protein association.

In reciprocal experiments, full-length and truncated versions of mPARP-2 fused to GST were expressed in HeLa cells and affinity-purified on glutathione-Sepharose beads. Copurification of endogenous PARP-1 was efficient with full-length mPARP-2 and with its E domain (Fig. 4*B*, *lanes 2* and *4*, respectively). These results showed that the E domain of PARP-2 is involved in both the homodimerization of PARP-2 (Fig. 2) and the heterodimerization with PARP-1 (Fig. 4*B*).

*PARP-2 and PARP-1 Poly(ADP-ribosyl)ate Each Other in Vitro*—The ability of PARP-1 to poly(ADP-ribosyl)ate PARP-2 was evaluated. Truncated versions of mPARP-2 fused to GST and expressed in HeLa cells were isolated on glutathione-Sepharose beads as described above for Fig. 4*B*, except that the

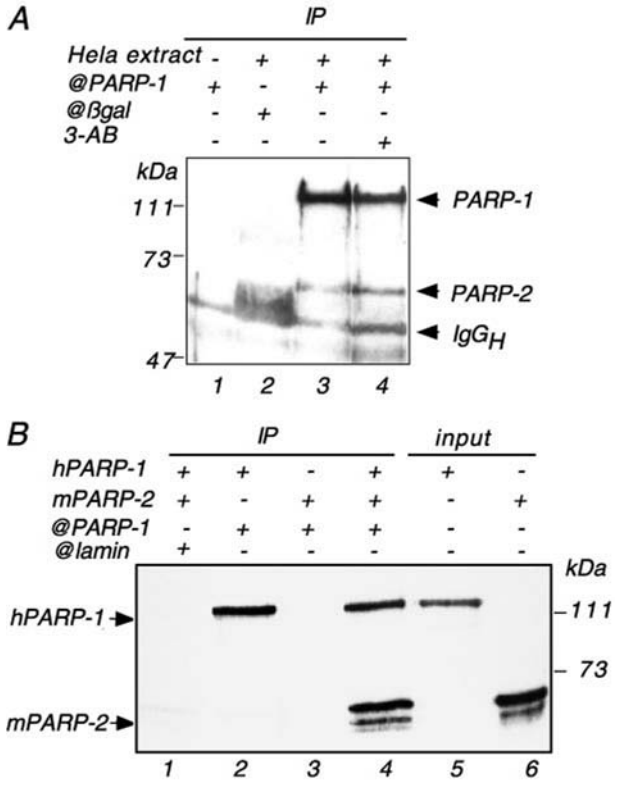


FIG. 3. **PARP-2 interacts with PARP-1 *in vitro* and *in vivo*.** *A*, co-immunoprecipitation of PARP-2 with PARP-1 in HeLa cell extracts. Extracts from untreated (*lanes 2* and *3*) or 1 mM 3-AB treated (*lane 4*) HeLa cells were incubated with the F1.23 mouse monoclonal anti-PARP-1 antibody (*lanes 3* and *4*) or with anti β-galactosidase antibody (*lane 2*). Bound immune complexes were analyzed by Western blot with a mixture of anti-PARP-1 and anti-PARP-2 polyclonal antibodies. *Lane 1*, control immunoprecipitation without HeLa extract. *B*, coimmunoprecipitation of purified mPARP-2 with purified hPARP-1. 1 μg of hPARP-1 (*lanes 1*, *2*, and *4*) was incubated without (*lanes 2* and *3*) or with 1 μg of mPARP-2 (*lanes 1* and *4*) and with either F1.23 anti PARP-1 (*lanes 2*, *3*, and *4*) or with anti-lamin (*lane 1*) monoclonal antibodies. Bound immune complexes were analyzed by Western blot as in *A*. *Inputs*: hPARP-1 (40 ng) and mPARP-2 (20 ng).

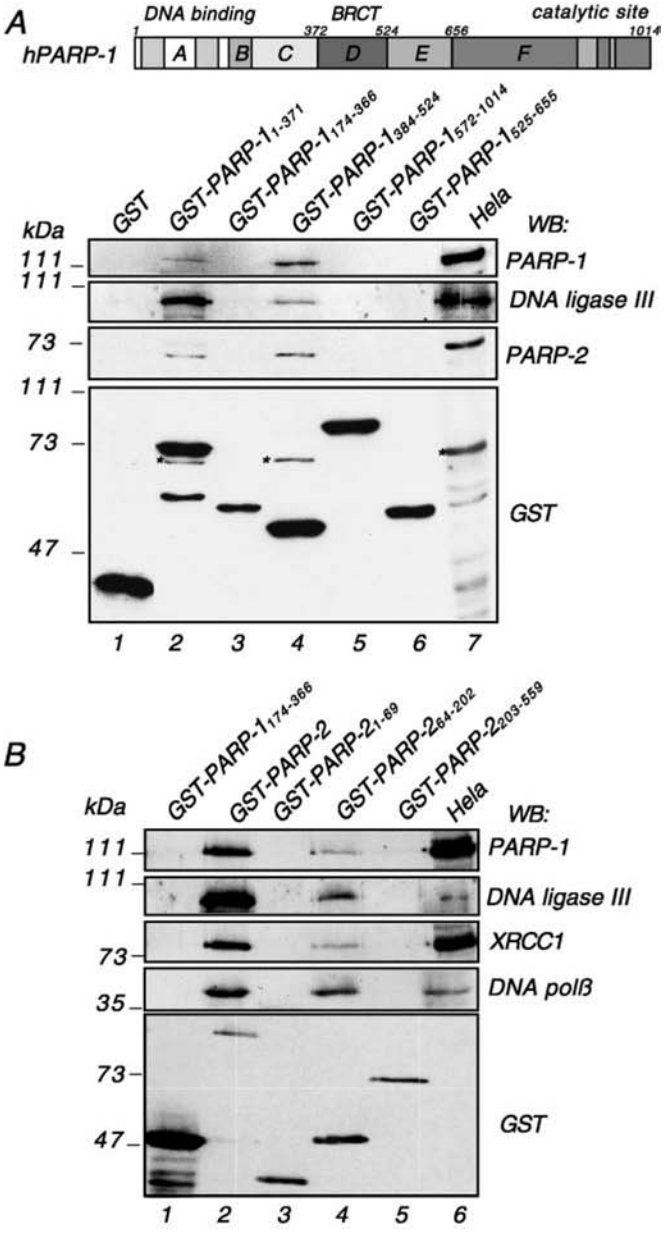


FIG. 4. **Interaction between PARP-2 and PARP-1: mapping of the interface domains.** *A*, schematic representation of hPARP-1. GST (*A* and *B*, *lane 1*) and GST-tagged deletion mutants of hPARP-1 (*A*, *lanes 2–6*) or mPARP-2 (*B*, *lanes 2–5*) were expressed in HeLa cells and interacting endogenous proteins were extracted by GST-pull-down and analyzed by Western blot, using the indicated antibodies. Blots were subsequently probed with anti-GST antibody (*A* and *B*, *bottom*: one representative GST immunodetection). *A*, *lane 7* and *B*, *lane 6*: crude extract of $4 \times 10^5$ HeLa cells. In *panel A*, the *stars* show the immunodetection of PARP-2 that was carried out before GST immunodetection.

washing buffer used contained 0.5 M NaCl and 0.5% Nonidet P-40 to prevent the interaction between endogenous PARP-1 and mPARP-2 (data not shown). Trapped proteins on the beads were incubated for 4 min with either hPARP-1 or mPARP-2 or neither, in the presence of [$^{32}$P]NAD (0.1 μM for hPARP-1 and 1 μM for mPARP-2 or control) and DNase I activated calf thymus DNA. Autoradiography revealed that hPARP-1 was able to poly-(ADP-ribosyl)ate the E domain of mPARP-2 (Fig. 5*A*, *panel 3*), and to a lesser extent the DNA binding domain (*panel 2*). Automodification of mPARP-2 was weakly detected only on the E domain (*panel 3*). In the presence of 3-AB, no auto-/heteromodification of the E domain of mPARP-2 was observed (*panel 5*), confirming that the radioactive labeling detected was due to polymer synthesis.

The reciprocal experiment showed that, in the presence of 1 μM [$^{32}$P]NAD, mPARP-2 poly(ADP-ribosyl)ates the DNA binding domain and the BRCT domain of hPARP-1 (Fig. 5*B*, *panels 1* and *3*, respectively). These domains contain most of the polymer acceptor sites in the automodification reaction of PARP-1 (Fig. 5*B*).

These results show that PARP-1 and PARP-2 can associate to form homo- or heterodimers and can be reciprocally poly-(ADP-ribosyl)ated.

*PARP-2 Belongs to a BER Complex Containing XRCC1, PARP-1, DNA polβ, and DNA Ligase III*—Given that PARP-1 is involved in base excision repair through its association with the scaffold protein XRCC1 (2–4), we examined whether PARP-2 and XRCC1 could also interact. The Western blot used to delineate the region of PARP-2 interacting with PARP-1 (described in Fig. 4*B*) was probed with the anti-XRCC1 antibody. Results showed that full-length mPARP-2 (Fig. 4*B*, *lane 2*) and its E-domain (*lane 4*) interacted with endogenous XRCC1, demonstrating that PARP-2 belongs to the BER complex through its interaction with XRCC1. A similar approach was used to identify the region of human XRCC1 (hXRCC1) interacting with PARP-2. Fig. 6*A* shows that only the GST fusion proteins harboring the central BRCT domain (BRCT1) of human XRCC1 (*lanes 3* and *4*) could interact with endogenous PARP-2. Neither the second BRCT of hXRCC1 (BRCT2) nor the N-terminal part of hXRCC1 known to interact with DNA polβ

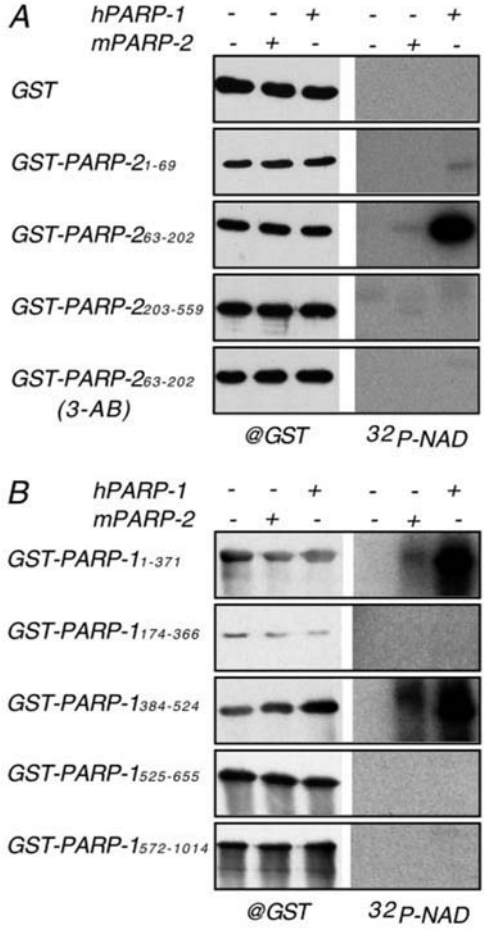


FIG. 5. **Heteromodification of PARP-1 and PARP-2.** The GST-tagged deletion mutants of mPARP-2 (*A*) or hPARP-1 (*B*) were expressed in HeLa cells, extracted by GST pull-down, and incubated 4 min at 25 °C in activity buffer with or without purified hPARP-1 or mPARP-2 as indicated in the presence of [$^{32}$P]NAD (1 $\mu$M for control and mPARP-2, 0.1 $\mu$M for hPARP-1) and DNase I activated DNA. Samples were analyzed by Western blot with anti-GST antibody (*left panels*) and autoradiography (18-h exposure at −80 °C, *right panels*). *A*, *bottom panel*: 1 mM 3-AB was present throughout the experiment.

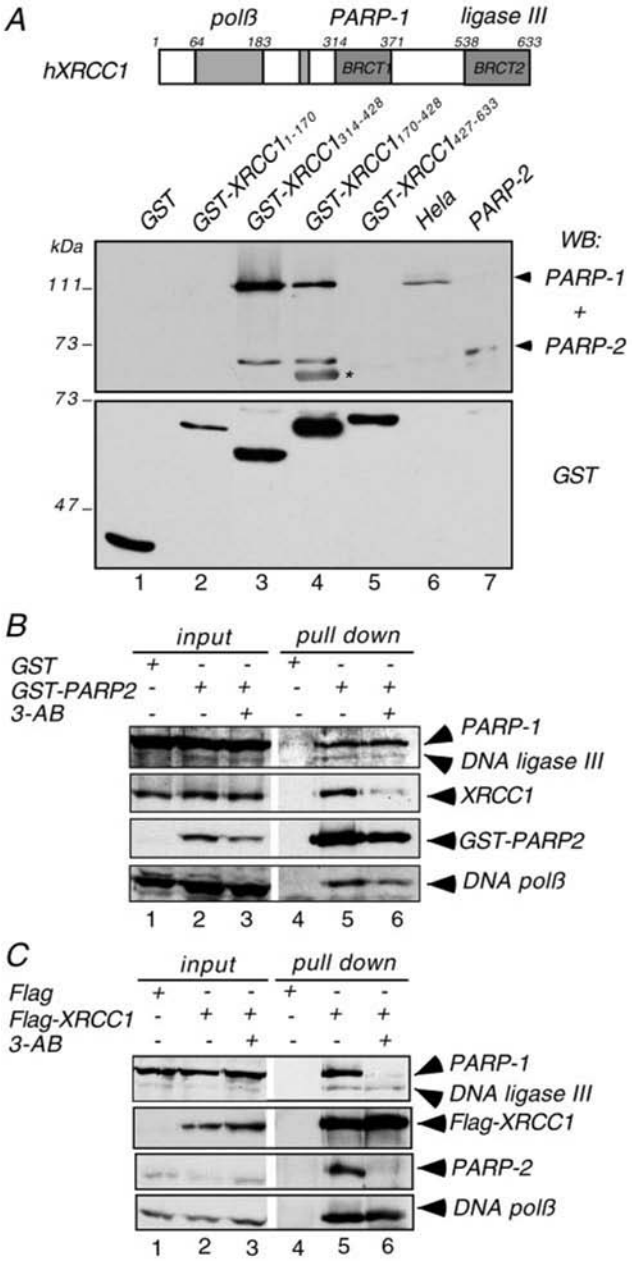


FIG. 6. **PARP-2 interacts with XRCC1.** *A*, proteins interacting with GST (*lane 1*) or GST-tagged deletion mutants of hXRCC1 (*lanes 2–5*) were extracted from HeLa cells by GST-pull-down and analyzed by Western blot with anti-PARP-2 and anti-PARP-1 antibodies (*top*: overlay of the two immunodetection signals. The *star* indicates a cross-reaction of anti-PARP-2 antibody with the GST-XRCC$_{1170-428}$ fusion protein). Blot was subsequently probed with anti-GST antibody (*bottom*). *Lane 6*, Crude extract of $2 \times 10^5$ HeLa cells and *lane 7*, 10 ng of purified mPARP-2. *B*, GST (*lanes 1* and *4*) or GST-mPARP-2 (*lanes 2*, *3*, *5*, and *6*) was expressed in HeLa cells, and interacting proteins were selectively extracted by GST-pull-down and analyzed by Western blot, using successively the indicated antibodies. Blot was subsequently probed with anti-GST antibody (*boldface*). *Lanes 3* and *6*, 1 mM 3-AB was present throughout the experiment. *Input* corresponds to 1/50 of the total cell extract used for the GST pull-down experiment. *C*, control FLAG (*lanes 1* and *4*) or FLAG-hXRCC1 (*lanes 2*, *3*, *5*, and *6*) was expressed in HeLa cells and immunoprecipitated with anti-FLAG antibody. Interacting proteins were analyzed by Western blot using successively the indicated antibodies. Blot was subsequently probed with anti-XRCC1 antibody (*boldface*) to detect the immunoprecipitated FLAG-hXRCC1 protein. *Lanes 3* and *6*, 1 mM 3-AB was present throughout the experiment. *Input* corresponds to 1/50 of the total cell extract used for the immunoprecipitation.

were found associated to PARP-2 (*lanes 2* and *5*, respectively). Therefore, XRCC1 interacts with both PARP-1 and PARP-2 through the same region, the BRCT1 module. The association between PARP-2 and XRCC1 resists stringent conditions (500 mM NaCl), indicating a high affinity of one protein for the other (data not shown).

DNA pol$\beta$ (4) and DNA ligase III (Fig. 4*A*) are other BER partners that interact with PARP-1. We tested whether these BER factors were associated with mPARP-2 by probing the Western blot described in Fig. 4*B* with anti-DNA ligase III and anti-DNA pol$\beta$ antibodies. Results showed that both DNA ligase III and DNA pol$\beta$ were trapped with full-length mPARP-2 and with its E domain, implying that PARP-2 belongs to a multiprotein BER complex containing at least PARP-1, XRCC1, DNA pol$\beta$, and DNA ligase III.

To examine whether the interactions between all these repair factors are regulated by poly(ADP-ribosyl)ation, we performed a GST pull-down analysis with mPARP-2 fused to GST expressed in HeLa cells in the presence or absence of 1 mM 3-AB (Fig. 6*B*). The interaction between mPARP-2 and either PARP-1 or DNA ligase III was independent of poly(ADP-ribose) synthesis. PARP's inhibition led to a slight decrease in PARP-2/DNA pol$\beta$ interaction and to a significant inhibition of PARP-2/XRCC1 interaction (Fig. 6*B*, compare *lanes 5* and *6*). A recip-

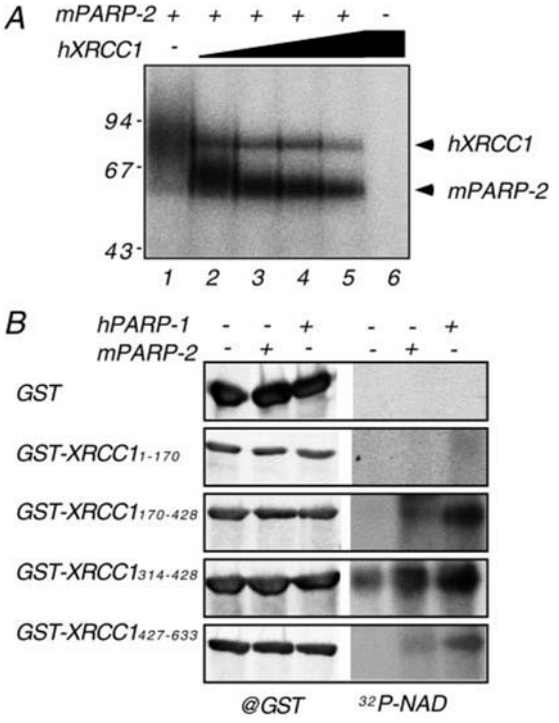


FIG. 7. **Poly(ADP-ribosyl)ation of XRCC1 and negative regulation of PARP-2.** *A*, purified mPARP-2 (200 pmol, *lanes 1–5*) were incubated with 0 (*lane 1*), 200 (*lane 2*), 400 (*lane 3*), 800 (*lane 4*), or 1600 (*lanes 5* and *6*) pmol of purified hXRCC1 for 2 min at 25 °C as described under "Experimental Procedures." Reaction products were analyzed by 8% gel electrophoresis and autoradiography of the Coomassie Blue-stained and dried gel. *B*, the GST-tagged deletion mutants of hXRCC1 were expressed in HeLa cells and analyzed as described in Fig. 5.

rocal experiment was performed, with the expression of the FLAG-tagged full-length hXRCC1 in HeLa cells and immunoprecipitation of this recombinant protein in the presence or absence of 1 mM 3-AB (Fig. 6*C*). Results showed that the association between hXRCC1 and DNA ligase III or DNA pol$\beta$ was not significantly affected by PARPs inhibition, whereas the interaction between hXRCC1 and both PARP-1 and PARP-2 was abolished by PARP's inhibition (Fig. 6*C*, compare *lanes 5* and *6* and *4*) indicating that polymer synthesis is a prerequisite for XRCC1 binding to PARP-2 as well as to PARP-1.

*XRCC1 Negatively Regulates PARP-2 Activity*—XRCC1 was shown both *in vitro* and *in vivo* to negatively regulate PARP-1 activity, by limiting PARP-1 automodification (3), forcing it to reside on the damaged DNA. The same effect was observed for PARP-2 in an *in vitro* poly(ADP-ribosyl)ation assay containing mPARP-2, DNase I-activated DNA, and [$^{32}$P]NAD (Fig. 7*A*). Increasing the concentration of purified recombinant His-tagged hXRCC1 (3) leads to the inhibition of mPARP-2 activity. This inhibition occurs even though hXRCC1 is a polymer acceptor of mPARP-2, as shown by the radioactive labeling corresponding to poly(ADP-ribosyl)ated hXRCC1. Thus, as for PARP-1, XRCC1 limits PARP-2 automodification.

To determine the polymer binding sites on XRCC1, truncated versions of hXRCC1 fused to GST were expressed in HeLa cells and purified on glutathione-Sepharose beads at high stringency and in the presence of 3-AB, to avoid copurification of endogenous PARP-1 and PARP-2 (see Fig. 5*B* and Ref. 3). The beads were incubated for 4 min with either hPARP-1 or mPARP-2 or neither PARP, in the presence of [$^{32}$P]NAD (1 $\mu$M for control and mPARP-2, 0.1 $\mu$M for hPARP-1) and DNase I-activated calf thymus DNA. The autoradiography shown in Fig. 7*B* revealed that polymer binding sites were present in the C-terminal part, lying between residues 314 and 428 (corresponding to the BRCT1 domain, *panels 3* and *4*) and to a lesser extend between residues 427 and 633 (encompassing the BRCT2 domain, *panel 5*). These polymer binding sites are functional for both mPARP-2 and hPARP-1. These results indicate that hXRCC1 is mainly poly(ADP-ribosyl)ated on the BRCT domain that interacts with PARP-1 and PARP-2. The C-terminal region of hXRCC1 encompassing the BRCT2 domain that interacts with DNA ligase III could also be poly(ADP-ribosyl)ated, in contrast to the N-terminal part that showed no polymer binding sites (*panel 2*). These results suggest that poly(ADP-ribosyl)ation of hXRCC1 regulates its interaction with PARP-1 and PARP-2. The interaction between hXRCC1 and DNA ligase III was not affected by the inhibition of PARP activity (see Fig. 6*C*), therefore the function of the poly(ADP-ribosyl)ation of the C-terminal part of hXRCC1 is still unclear. In addition to PARP-1, PARP-2, DNA pol$\beta$, and DNA ligase III, XRCC1 has been shown to associate other partners in BER such as APE1 (33) and PNK (34). We hypothesize that poly(ADP-ribosyl)ation of the C-terminal part of XRCC1 may regulate its association with one (or more) of these.

*PARP-2 Is Required for Efficient DNA Repair of Alkylated DNA in Vivo*—The presence of PARP-2 in a BER complex containing at least PARP-1, XRCC1, DNA pol$\beta$, and DNA ligase III strongly supports a role of PARP-2 in this DNA repair pathway. We have generated mice deficient in PARP-2 by inactivation of exon 9 of the PARP-2 gene by homologous recombination.[2] Mouse embryonic fibroblasts (MEFs) were prepared from 13.5 d.p.c. embryos. Western blot analyses of crude extracts from these MEFs at passage 2 were performed using several polyclonal anti-PARP-2 antibodies raised against full-length mPARP-2 or its catalytic domain. These antibodies recognized PARP-2 in PARP-2$^{+/+}$ and PARP-2$^{+/-}$ cells, but failed to detect any PARP-2 or truncated fragment of it in PARP-2$^{-/-}$ cells (Fig. 8A, lower panel and data not shown). The same blot was probed with the anti-PARP-1 antibody (Fig. 8A, *upper panel*), showing the presence of PARP-1 at comparable levels in MEFs from any genotype, indicating no deregulation of PARP-1 expression in the PARP-2 deficient cells.

To evaluate the contribution of PARP-2 to PARP activity, we measured the polymer formation in whole cell extracts from PARP-2$^{+/+}$, PARP-2$^{-/-}$, and PARP-1$^{-/-}$ passage 3 MEFs (Fig. 8*B*). Results showed that *in vitro* poly(ADP-ribose) synthesis stimulated by DNA strand breaks was only moderately affected in PARP-2$^{-/-}$ cells compared with PARP-2$^{+/+}$ cells, as opposed to the severe inhibition of polymer synthesis in PARP-1$^{-/-}$ cells (15). Immunofluorescence analyzes using the 10H monoclonal antibody raised against poly(ADP-ribose) showed no evident decrease in polymer synthesis in PARP-2$^{-/-}$ cells treated with 1 mM $H_2O_2$ or 2 mM MNU compare with PARP-2$^{+/+}$ cells (data not shown). These observations demonstrate that the absence of PARP-2 has only a weak effect on the total PARP activity stimulated by DNA breaks.

The capacity of PARP-2$^{-/-}$ cells to repair DNA lesions induced by alkylating agents was evaluated *in vivo* using the single-cell gel electrophoresis assay (COMET assay) and compared with that of PARP-2$^{+/+}$, PARP-1$^{+/+}$, and PARP-1$^{-/-}$ cells. Passage 3 MEFs of the four genotypes were exposed to MNU for 30 min as indicated in Fig. 8*C*, or mock treated. Measurement of the COMET tail moment reflecting the level of DNA fragmentation (27) revealed that DNA breakage varied in a linear manner with increasing doses of MNU in the range of 0–1 mM for each genotype (data not shown). A repair assay performed with 1 mM MNU showed that PARP-2$^{-/-}$ cells dis-

[2] J. Ménissier-de Murcia *et al.*, manuscript in preparation.

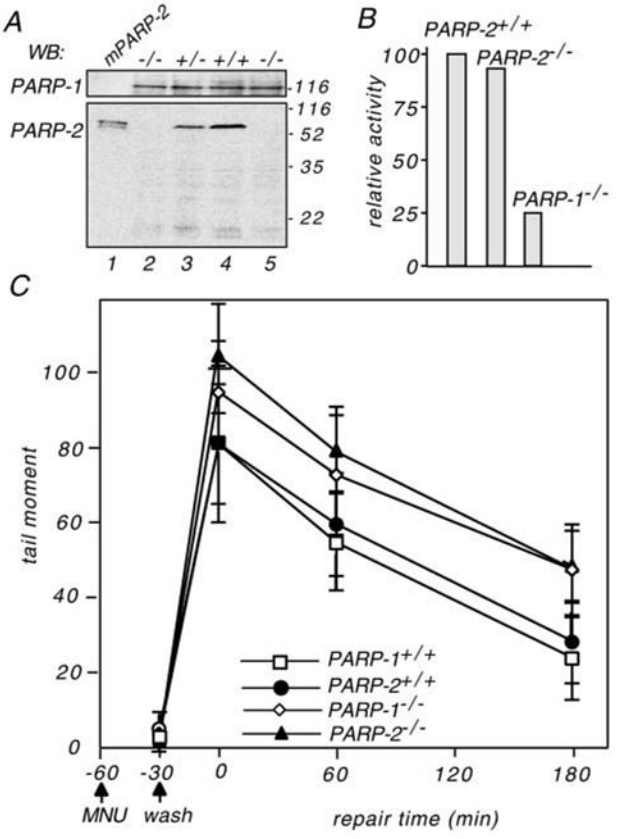


FIG. 8. **DNA repair capacity of PARP-2$^{+/+}$, PARP-2$^{-/-}$, PARP-1$^{+/+}$, and PARP-1$^{-/-}$ MEFs treated with MNU as assessed by the COMET assay.** *A*, Western blot analysis of total cell extract from passage 2 primary MEFs derived from 13.5 d.p.c. embryos resulting from intercrosses between PARP-2$^{+/-}$ mice. The blot was sequentially probed with anti-PARP-2 (*lower panel*) and anti-PARP-1 (*upper panel*) polyclonal antibodies. *B*, relative PARP activity in PARP-2$^{+/+}$, PARP-2$^{-/-}$, and PARP-1$^{-/-}$ passage 3 primary MEFs. Cell extracts were incubated in standard conditions with [$^{32}$P]NAD and DNase I-activated DNA for 10 min at 25 °C. Activity is expressed as the percentage of the radioactivity of acid-insoluble material produced by cell extracts compared with PARP-2$^{+/+}$ cell extract. *C*, kinetic of re-ligation of DNA breaks induced by treatment of passage 4 MEFs cells (PARP-1$^{+/+}$, *squares*; PARP-2$^{+/+}$, *circles*; PARP-2$^{-/-}$, *triangles*; and PARP-1$^{-/-}$, *diamonds*) with 1 mM MNU for 30 min. The distribution of the tail moment as a function of repair time is indicated. The results shown are representative of one out of three experiments.

played a considerably slower rejoining kinetic (a 2-h delay in DNA strand breaks resealing) compared with PARP-2$^{+/+}$ and PARP-1$^{+/+}$ cells, but similar to that observed for PARP-1$^{-/-}$ cells (Fig. 8*C*). These results unambiguously show that, despite the presence of PARP-1, PARP-2$^{-/-}$ cells are defective in BER, demonstrating the requirement of PARP-2 for efficient DNA strand break resealing.

## DISCUSSION

*Similar Expression Pattern of PARP-1 and PARP2 Genes*—In this study, we showed that the expression of the *PARP-1* and *PARP-2* genes were almost similar, both being ubiquitously expressed at all stages of mouse development and in adult tissues, with variable levels and with a generally weaker intensity for *PARP-2* compared with *PARP-1*. Expression of both transcripts seemed to be correlated with proliferation, with higher levels occurring during early fetal development and organogenesis and in the highly proliferative cell compartments of adult mice. It is conceivable that cells undergoing intensive division need functional DNA damage sensing and repair factors to avoid inherited genomic alterations. Interestingly, we observed that murine tumors also displayed high expression of both *PARP-1* and *PARP-2* compared with normal tissue (data not shown). *PARP-1* and *-2* cannot be exclusively considered as genes expressed in highly proliferating cells, because high expression of both genes was also detected in the post-mitotic neurons of cranial and spinal ganglia, in hippocampal pyramidal cell layers, and in the dentate gyrus of the brain, although the two latter are known to contain progenitor neuronal cells (35). Several genes involved in DNA damage sensing and repair have been reported to be expressed in neuronal cell lines, such as ATM (36), p53 (37), T:G mismatch-specific thymidine-DNA glycosylase (38), and APE1 (39), because these cells need to be efficiently protected from DNA injury.

*PARP-1 and PARP-2 Heterodimerize*—The almost similar tissue distribution of PARP-1 and PARP-2 raises the question of why eukaryotic cells need simultaneously two DNA damage-dependent PARPs. The requirement of a functional PARP-1/PARP-2 heterodimer could be a plausible hypothesis. In this study, we demonstrated that PARP-2 and PARP-1 homo- or heterodimerize and heteromodify each other. The PARP-2 E domain appears to act as a protein/protein interface regulated by auto- or heteromodification. Interestingly this domain is enriched in glutamate residues that are potential automodification sites. Despite a significant amino acid sequence conservation (38% identity, 47% similarity), the PARP-1 E domain displays none of these properties, unlike the neighboring BRCT motif. It seems likely that the E domain of PARP-2 combines the properties of the D and E domains of PARP-1.

At the cellular level, both enzymes reside in the nucleus and colocalize partially into the nucleolus (40).[3] This distribution suggests the need for heterodimers in the nucleolar compartment where repetitive sequences (rDNA) need to be particularly protected.

Clearly, the biological significance of PARP-1/PARP-2 heterodimerization needs to be further elucidated. Does PARP-2 (endowed with a low specific activity) need PARP-1 (the most active member of the family) at a DNA lesion to amplify the cellular response to DNA damage? Interestingly, a direct interaction between PARP-1 and PARP-3, in the centrosome compartment, has also recently been found,[4] suggesting a possible generalization of this observation to other PARP homologues. This type of organization of PARPs in physiological complexes would increase the number of possible partners, which in turn may adapt the responses of the cell to the nature of the injury and to the local environment.

*What Is the Function of PARP-2 in BER?*—It is more likely that both PARPs are required simultaneously to act in the same macromolecular base excision DNA repair complex. We and others have demonstrated the requirement of XRCC1, PARP-1, and DNA pol$\beta$ for both short patch (SPR) and long patch (LPR) BER pathways (2, 4, 9, 41–45). This new link between XRCC1 and PARP-2, observed only in the presence of polymer synthesis (as for the PARP-1/XRCC1 interaction) strongly suggests a concerted role of the PARP-1/PARP-2 heterodimer during base excision repair, most probably at the recruitment step of XRCC1 at damaged sites. The phenotype of embryonic fibroblasts derived from PARP-2 knockout mice displaying a severe delay in strand breaks resealing after MNU treatment, supports this point of view. Interestingly, the absence of PARP-2 is as dramatic as the absence of PARP-1. This observation was quite unexpected, because PARP-2 activity in response to DNA damage is about 10 times less than PARP-1 activity. However, if we assume that PARP-1 and PARP-2 have

[3] J.-C. Amé and V. Schreiber, manuscript in preparation.
[4] A. Augustin and C. Spenlehauer, manuscript in preparation.

to act as a heterodimer in base excision repair, then the absence of one of each would have the same consequence on repair efficiency.

Although more work is necessary to unravel the relative function of PARP-1 and PARP-2 in BER, the implication of the former in this pathway is becoming more evident. Two characteristic properties of PARP-1 place this enzyme at early steps of the repair process, most probably downstream from the action of DNA glycosylases and/or APE1: (i) detection and binding to the sugar-phosphate backbone interruption; (ii) bending of the nicked substrate by 100° (46) that generates a distorted structure, in turn, recognized by the next enzyme in the pathway (47). Both the ability of XRCC1 to bind the inside bend of DNA (48) and its increased affinity for oligo(ADP-ribosyl)ated PARP-1 and/or PARP-2 or polymers (this study and Refs. 3, 5) may contribute to organize a protein platform at the DNA break for additional BER enzymes: PNK, DNA pol$\beta$, and finally DNA ligase III (see for review Ref. 49). Additionally, we have shown that the polymerization step of LPR was mainly affected in PARP-1-deficient cells (4). Lavrik *et al.* (8) showed that PARP-1, associated to DNA pol$\beta$, efficiently binds to the repair intermediates containing a flap 5′-abasic site that are formed before sub-pathway choice leading to either SPR or LPR. The same group demonstrated that PARP-1, together with FEN-1, stimulates strand displacement synthesis by DNA pol$\beta$ (9) leading to LPR. The authors proposed that the dRP group might serve as a sensor for the recruitment of PARP-1 onto BER intermediates, then PARP-1 would activate long patch BER by recruiting other long patch repair proteins. It remains an open question whether PARP-2 is also bound to this dRP-containing repair intermediate along with PARP-1. It is also possible that PARP-2, either alone or together with PARP-1, is involved in a distinct step of the repair process. Because PARP-1 and PARP-2 DNA binding domains differ totally, we can assume that they may have distinct DNA targets. The elucidation of the specific DNA structures (repair intermediates) recognized by PARP-2 will undoubtedly help to elucidate at which step(s) of BER it is involved.

*Acknowledgments*—We thank Dr. Shanti Natarajan-Amé for critical reading of the manuscript. We are grateful to Prof. Pierre Chambon, Institut de Génétique et de Biologie Moléculaire et Cellulaire, Illkirch, France, for continual support.

REFERENCES

1. de Murcia, G., and Shall, S. (2000) *From DNA Damage and Stress Signalling to Cell Death*, Oxford University Press, Oxford
2. Caldecott, K., Aoufouchi, S., Johnson, P., and Shall, S. (1996) *Nucleic Acids Res.* **24,** 4387–4394
3. Masson, M., Niedergang, C., Schreiber, V., Muller, S., Ménissier-de Murcia, J., and de Murcia, G. (1998) *Mol. Cell. Biol.* **18,** 3563–3571
4. Dantzer, F., de La Rubia, G., Ménissier-De Murcia, J., Hostomsky, Z., de Murcia, G., and Schreiber, V. (2000) *Biochemistry* **39,** 7559–7569
5. Pleschke, J. M., Kleczkowska, H. E., Strohm, M., and Althaus, F. R. (2000) *J. Biol. Chem.* **275,** 40974–40980
6. Trucco, C., Oliver, F. J., de Murcia, G., and Ménissier-de Murcia, J. (1998) *Nucleic Acids Res.* **26,** 2644–2649
7. Beneke, R., Geisen, C., Zevnik, B., Bauch, T., Muller, W. U., Kupper, J. H., and Moroy, T. (2000) *Mol. Cell. Biol.* **20,** 6695–6703
8. Lavrik, O. I., Prasad, R., Sobol, R. W., Horton, J. K., Ackerman, E. J., and Wilson, S. H. (2001) *J. Biol. Chem.* **276,** 25541–25548
9. Prasad, R., Lavrik, O. I., Kim, S. J., Kedar, P., Yang, X. P., Vande Berg, B. J., and Wilson, S. H. (2001) *J. Biol. Chem.* **276,** 32411–32414
10. Wang, Z. Q., Auer, B., Stingl, L., Berghammer, H., Haidacher, D., Schweiger, M., and Wagner, E. F. (1995) *Genes Dev.* **9,** 509–520
11. Ménissier-de Murcia, J., Niedergang, C., Trucco, C., Ricoul, M., Dutrillaux, B., Mark, M., Olivier, F. J., Masson, M., Dierich, A., LeMeur, M., Walztinger, C., Chambon, P., and de Murcia, G. (1997) *Proc. Natl. Acad. Sci. U. S. A.* **94,** 7303–7307
12. Masutani, M., Nozaki, T., Nishiyama, E., Shimokawa, T., Tachi, Y., Suzuki, H., Nakagama, H., Wakabayashi, K., and Sugimura, M. (1999) *Mol. Cell. Biochem.* **193,** 149–152
13. Szabo, C. (2000) in *From DNA Damage and Stress Signalling to Cell Death* (de Murcia, G., and Shall, S., eds), pp. 151–176, Oxford University Press, Oxford.
14. Shieh, W. M., Ame, J. C., Wilson, M. V., Wang, Z. Q., Koh, D. W., Jacobson, M. K., and Jacobson, E. L. (1998) *J. Biol. Chem.* **273,** 30069–30072
15. Amé, J. C., Rolli, V., Schreiber, V., Niedergang, C., Apiou, F., Decker, P., Muller, S., Hoger, T., Ménissier-de Murcia, J., and de Murcia, G. (1999) *J. Biol. Chem.* **274,** 17860–17868
16. Berghammer, H., Ebner, M., Marksteiner, R., and Auer, B. (1999) *FEBS Lett.* **449,** 259–263
17. Johansson, M. (1999) *Genomics* **57,** 442–445
18. Kickhoefer, V. A., Siva, A. C., Kedersha, N. L., Inman, E. M., Ruland, C., Streuli, M., and Rome, L. H. (1999) *J. Cell Biol.* **146,** 917–928
19. Smith, S., Giriat, I., Schmitt, A., and de Lange, T. (1998) *Science* **282,** 1484–1487
20. Chi, N. W., and Lodish, H. F. (2000) *J. Biol. Chem.* **275,** 38437–38444
21. Kaminker, P. G., Kim, S. H., Taylor, R. D., Zebarjadian, Y., Funk, W. D., Morin, G. B., Yaswen, P., and Campisi, J. (2001) *J. Biol. Chem.* **276,** 35891–35899
22. Lyons, R. J., Deane, R., Lynch, D. K., Ye, Z. S., Sanderson, G. M., Eyre, H. J., Sutherland, G. R., and Daly, R. J. (2001) *J. Biol. Chem.* **276,** 17172–17180
23. Ma, Q., Baldwin, K. T., Renzelli, A. J., McDaniel, A., and Dong, L. (2001) *Biochem. Biophys. Res. Commun.* **289,** 499–506
24. Doucet-Chabeaud, G., Godon, C., Brutesco, C., de Murcia, G., and Kazmaier, M. (2001) *Mol. Genet. Genomics* **265,** 954–963
25. Chatton, B., Bahr, A., Acker, J., and Kedinger, C. (1995) *BioTechniques* **18,** 142–145
26. Niederreither, K., and Dollé, P. (1998) *Methods Mol. Biol.* **89,** 247–267
27. Olive, P. L., Banath, J. P., and Durand, R. E. (1990) *Radiat. Res.* **122,** 86–94
28. Pieper, A. A., Blackshaw, S., Clements, E. E., Brat, D. J., Krug, D. K., White, A. J., Pinto-Garcia, P., Favit, A., Conover, J. R., Snyder, S. H., and Verma, A. (2000) *Proc. Natl. Acad. Sci. U. S. A.* **97,** 1845–1850
29. Concha, I. I., Figueroa, J., Concha, M. I., Ueda, K., and Burzio, L. O. (1989) *Exp. Cell Res.* **180,** 353–366
30. Bauer, P. I., Buki, K. G., Hakam, A., and Kun, E. (1990) *Biochem. J.* **270,** 17–26
31. Mendoza-Alvarez, H., and Alvarez-Gonzalez, R. (1993) *J. Biol. Chem.* **268,** 22575–22580
32. Lamarre, D., Talbot, B., de Murcia, G., Laplante, C., Leduc, Y., Mazen, A., and Poirier, G. G. (1988) *Biochim. Biophys. Acta* **950,** 147–160
33. Vidal, A. E., Boiteux, S., Hickson, I. D., and Radicella, J. P. (2001) *EMBO J.* **20,** 6530–6539
34. Whitehouse, C. J., Taylor, R. M., Thistlethwaite, A., Zhang, H., Karimi-Busheri, F., Lasko, D. D., Weinfeld, M., and Caldecott, K. W. (2001) *Cell* **104,** 107–117
35. Gage, F. H., Kempermann, G., Palmer, T. D., Peterson, D. A., and Ray, J. (1998) *J. Neurobiol.* **36,** 249–266
36. Barlow, C., Ribaut-Barassin, C., Zwingman, T. A., Pope, A. J., Brown, K. D., Owens, J. W., Larson, D., Harrington, E. A., Haeberle, A. M., Mariani, J., Eckhaus, M., Herrup, K., Bailly, Y., and Wynshaw-Boris, A. (2000) *Proc. Natl. Acad. Sci. U. S. A.* **97,** 871–876
37. Schmid, P., Lorenz, A., Hameister, H., and Montenarh, M. (1991) *Development* **113,** 857–865
38. Niederreither, K., Harbers, M., Chambon, P., and Dollé, P. (1998) *Oncogene* **17,** 1577–1585
39. Wilson, T. M., Rivkees, S. A., Deutsch, W. A., and Kelley, M. R. (1996) *Mutat. Res.* **362,** 237–248
40. Desnoyers, S., Kaufmann, S. H., and Poirier, G. G. (1996) *Exp. Cell Res.* **227,** 146–153
41. Kubota, Y., Nash, R. A., Klungland, A., Barnes, D., and Lindahl, T. (1996) *EMBO J.* **23,** 6662–6670
42. Cappelli, E., Taylor, R., Cevasco, M., Abbondandolo, A., Caldecott, K., and Frosina, G. (1997) *J. Biol. Chem.* **272,** 23970–23975
43. Dianov, G. L., Prasad, R., Wilson, S. H., and Bohr, V. A. (1999) *J. Biol. Chem.* **274,** 13741–13743
44. Horton, J. K., Prasad, R., Hou, E., and Wilson, S. H. (2000) *J. Biol. Chem.* **275,** 2211–2218
45. Prasad, R., Dianov, G. L., Bohr, V. A., and Wilson, S. H. (2000) *J. Biol. Chem.* **275,** 4460–4466
46. Le Cam, E., Fack, F., Ménissier-de Murcia, J., Cognet, J. A., Barbin, A., Sarantoglou, V., Revet, B., Delain, E., and de Murcia, G. (1994) *J. Mol. Biol.* **235,** 1062–1071
47. Mol, C. D., Izumi, T., Mitra, S., and Tainer, J. A. (2000) *Nature* **403,** 451–456
48. Marintchev, A., Mullen, M. A., Maciejewski, M. W., Pan, B., Gryk, M. R., and Mullen, G. P. (1999) *Nat. Struct. Biol.* **6,** 884–893
49. Caldecott, K. W. (2001) *Bioessays* **23,** 447–455